



This open access document is posted as a preprint in the Beilstein Archives at <https://doi.org/10.3762/bxiv.2022.52.v1> and is considered to be an early communication for feedback before peer review. Before citing this document, please check if a final, peer-reviewed version has been published.

This document is not formatted, has not undergone copyediting or typesetting, and may contain errors, unsubstantiated scientific claims or preliminary data.

Preprint Title Effects of focused electron beam irradiation parameters on direct nanostructure formation on Ag surfaces

Authors Jānis Sniķeris, Vjačeslavs Gerbreders, Andrejs Bulanovs and Ēriks Sļedevskis

Publication Date 21 Jun 2022

Article Type Full Research Paper

ORCID® IDs Jānis Sniķeris - <https://orcid.org/0000-0002-5618-9741>

License and Terms: This document is copyright 2022 the Author(s); licensee Beilstein-Institut.

This is an open access work under the terms of the Creative Commons Attribution License (<https://creativecommons.org/licenses/by/4.0>). Please note that the reuse, redistribution and reproduction in particular requires that the author(s) and source are credited and that individual graphics may be subject to special legal provisions.

The license is subject to the Beilstein Archives terms and conditions: <https://www.beilstein-archives.org/xiv/terms>.

The definitive version of this work can be found at <https://doi.org/10.3762/bxiv.2022.52.v1>

Effects of focused electron beam irradiation parameters on direct nanostructure formation on
Ag surfaces

J. Sņiķeris*, V. Gerbreders, A. Bulanovs, E. Sņedevskis

Daugavpils University, Institute of Life Sciences and Technologies

Parādes Str. 1, Daugavpils, LV-5401, LATVIA

*e-mail: janis.snikeris@du.lv

Keywords: electron beam; nanostructure; silver; surface; atomic force microscopy.

Abstract

Metallic nanostructures have many applications, including photonics and plasmonics due to their ability to absorb or emit light at frequencies which depend on their size and shape. It was recently shown that irradiation by a focused electron beam can promote nanostructure growth on metal surfaces and the height of these structures depends on irradiation time and material of the surface. However, the effects on growth dynamics of numerous irradiation parameters, such as beam current or angle of incidence, have not yet been studied in detail. In this work, we explore the effects of the focusing, the angle of incidence, and the current of the electron beam on the size and shape of the resulting structures on an Ag surface, as well as investigating how the nitrogen plasma cleaning procedure of a vacuum chamber can affect the growth of these structures. A beam current of around 40 pA resulted in the fastest structure growth rate. Increasing the beam diameter and angle of incidence decreased the growth rate, but raising the beam focus up to 5-6 μm above the surface increased it. The vacuum chamber cleaning reduced the structure's growth rate for a few hours. These findings can help better control and optimise the nanostructure growth on metal surfaces undergoing irradiation by a focused electron beam.

Introduction

Metallic nanostructures have various uses, including in nano-electro-mechanical systems [1], plasmonic biosensors [2], and nano-photonics [3]. They can also serve as catalysts for controlled chemical vapour deposition [4].

Electron beam (EB) lithography is a popular method for the nano-patterning of metal surfaces, but it is a complicated and expensive multi-step process [5]. It has been shown that nanostructures can be directly grown on metal surfaces by EB irradiation in a single fabrication step without resist layers or etching [6, 7], and their height depends on the irradiation time and melting point of the surface metal; a lower melting point results in higher structures. It has also been observed that metal surfaces with a higher magnetic susceptibility produce wider structures. Partially reversible nanostructures were recently produced on the surface of a shape memory NiTi alloy using focused EB irradiation [8]. The volume of those nanostructures decreased by up to 88% upon heating the NiTi surface to 100°C from room temperature, while their height remained unchanged. However, it is still unclear how several irradiation parameters, such as the beam focusing, beam current, and angle of incidence, affect the growth process of nanostructures on metal surfaces under focused EB irradiation.

Hydrocarbon contamination from samples and vacuum pump oils are known to be ever-present in the vacuum chambers of electron microscopes [9]. Its presence is difficult to control and practically impossible to eliminate completely, but it can be reduced by plasma cleaning procedures. The formation of carbon nanopillars from the EB-induced deposition of free hydrocarbons in a scanning electron microscope (SEM) vacuum chamber has previously been reported [10]. It is important to evaluate if the presence of hydrocarbons affects the growth dynamics of nanostructures subjected to irradiation by focused EB.

In this work, we sought to observe how changing individual irradiation parameters (beam current, focusing, angle of incidence, and presence of hydrocarbons) affects the growth of nanostructures on Ag surfaces undergoing irradiation by focused EB in point mode.

Experimental setup

The samples were prepared by sputtering 500 nm thick Ag layers on Si(111) substrates via direct current (DC) magnetron sputtering. The surface of the samples was irradiated with a focused EB with controlled parameters in point mode using a “Tescan MAIA3” SEM (Figure 1a). Several samples were irradiated, each time changing one of

irradiation parameters and keeping the other parameters constant. Following irradiation, the shapes and sizes of the structures formed in irradiated points were determined by non-contact atomic force microscopy (AFM) using the “Park NX10” AFM model.

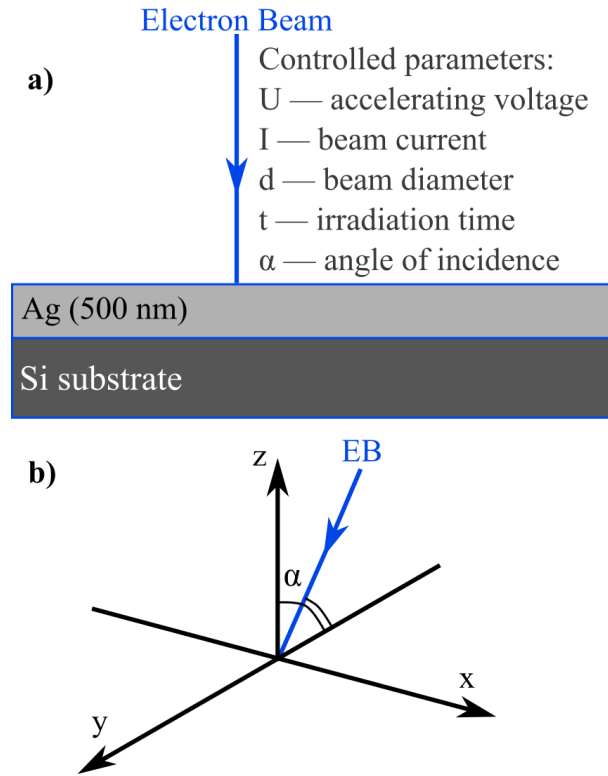


Figure 1: **a)** Structure of samples and experimental setup of their irradiation. **b)** Coordinate system for the angle of incidence of the electron beam (EB); the surface of the samples is along the xy plane, and the angle of incidence is in the yz plane.

The first experiment was conducted with beam current I as the variable parameter in a range from 7 to 500 pA. However, changing the value of I also changed the beam diameter d, which is a function of I and working distance (WD). The value of WD was adjusted to maintain a constant d while changing I. Since the range of WD was limited by the movement of the SEM stage, it was impossible to fit the whole range of I in a single d value without a risk of hitting sample with the electron gun, and therefore, this measurement was split into two separate d values – 10 and 15 nm.

The second experiment focused on testing the effects of the displacement of the EB focus above or below the surface of the sample. This was done by focusing the EB on the

surface of the sample and moving the SEM stage along the z axis for different points of irradiation.

The third experiment explored how the angle of incidence α of EB could affect the formation of nanostructures on an Ag surface. The value of α was changed by tilting the SEM stage. The position of EB relative to the sample surface is illustrated in Figure 1b. The EB was tilted along the yz plane over a range from 0 to 50° and irradiation was carried out with different α values along the x axis. The EB was refocused on the surface of the sample every time the α value was changed.

The fourth and last experiment considered the effects of hydrocarbon contamination in the vacuum chamber on the formation of nanostructures. This was done by irradiating the Ag surface with a focused EB before and after the nitrogen (N) plasma cleaning procedure in the SEM vacuum chamber. The procedure lasted 5 min and the applied power was 20 W. The time was counted from the end of the cleaning procedure. The sample had to be removed from the vacuum chamber during the cleaning procedure, because the N plasma cleaning procedure affected the Ag surface, most notably by forming a layer, which produces thin film interference. The sample irradiation was repeated 15 min, 30 min, 1 h, and 2 h after the end of the cleaning procedure.

Results

Figure 2 shows how the current and diameter of the EB affect the growth of nanostructures on an Ag surface. Over the EB current range of up to around 40 pA, the height of the nanostructures sharply increased up to 140 nm with the increase of beam current when the beam diameter was 15 nm. When the EB current increased beyond 40 pA the height of the nanostructures started decreasing at a slightly slower rate. Decreasing the EB diameter from 15 nm to 10 nm increased the height of the structures from 135 to 162 nm at an EB current value of 50 pA. Increasing the EB current value further from 50 to 500 pA resulted in a gradual decrease of the structure heights from 162 to 64 nm if the beam diameter was 10 nm.

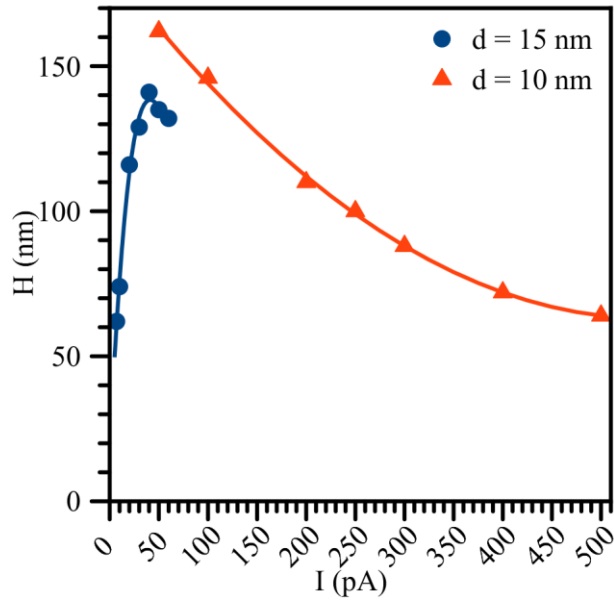


Figure 2: The height of nanostructures on an Ag surface as a function of the electron beam (EB) current I and diameter d . Constant beam parameters: $U = 30$ kV; $t = 40$ s; $\alpha = 0^\circ$.

Figure 3 shows the results of the EB focus displacement above and below the surface of the Ag sample. When the focus of the EB was displaced under the surface of the sample, the height of the nanostructures gradually decreased from 200 nm to around 110 nm, as displacement reached 6 μm below the surface. When the focus was displaced above the surface, the height of the nanostructures increased up to around 230 nm, as displacement reached 5-6 μm above the surface. If the focus of the EB was displaced to more than 6 μm above the surface, the height of the nanostructures started decreasing again.

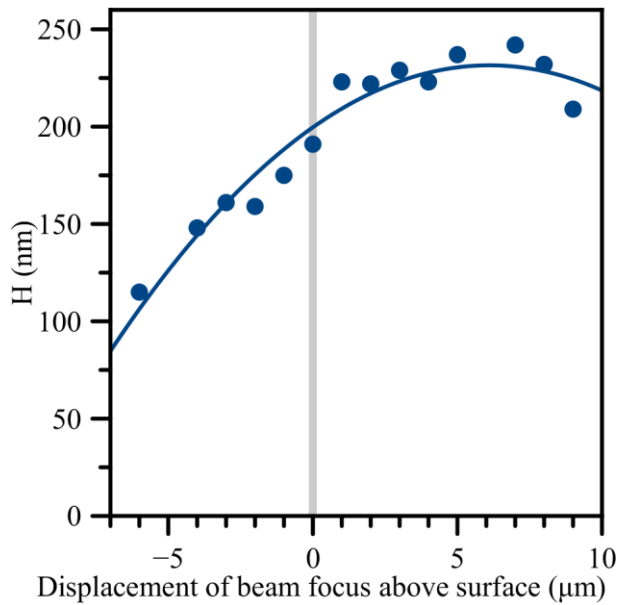


Figure 3: The height of the nanostructures on an Ag surface as a function of the displacement of the electron beam (EB) focus relative to the surface. Constant EB parameters: $U = 30$ kV; $I = 40$ pA; $d = 10$ nm; $t = 60$ s; $\alpha = 0^\circ$.

The results about the effects of changing the angle of incidence of the EB are presented in Figures 4 and 5. The main effect observed was the decrease of nanostructure height from 200 to 60 nm, as the angle of incidence increased up to 50° (Figure 4). We expected to observe a displacement of the nanostructures' peaks towards the direction of the EB as the angle of incidence was increased, but Figure 5 shows this did not happen. When comparing structures with α values of 0° and 10° , the peak of the nanostructure with $\alpha = 10^\circ$ was actually slightly displaced in the opposite direction.

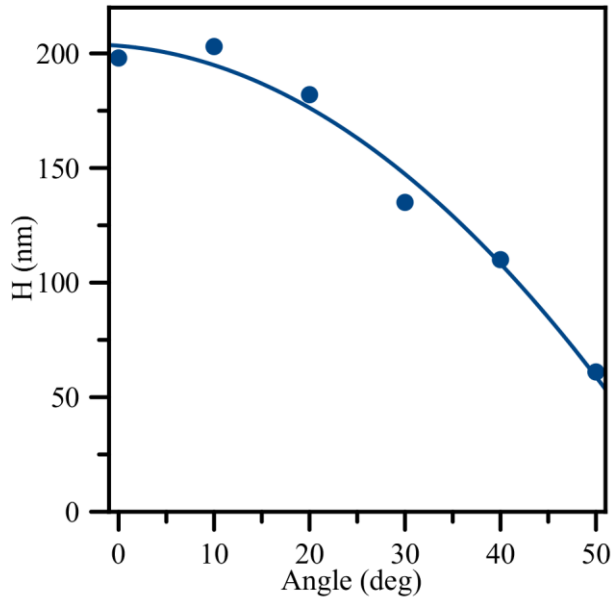


Figure 4: The height of the nanostructures on an Ag surface as a function of the angle of incidence of the electron beam (EB). Constant EB parameters: $U = 30$ kV; $I = 42$ pA; $d = 14$ nm; $t = 60$ s.

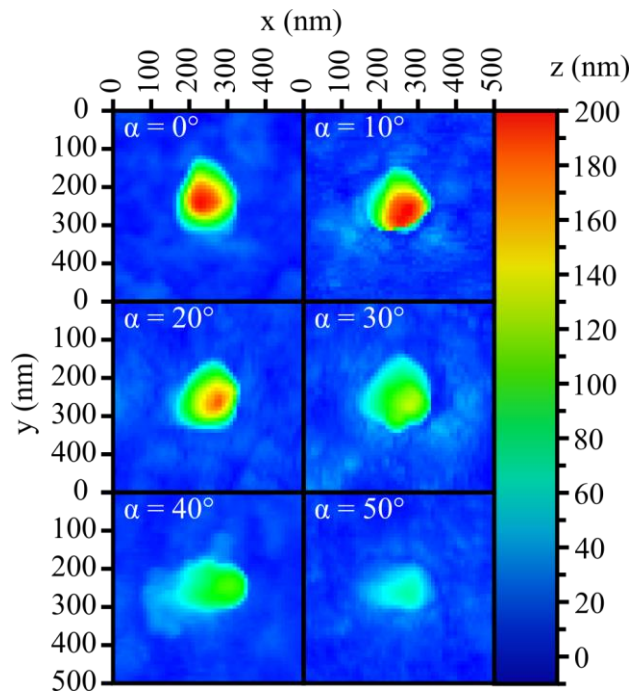


Figure 5: Atomic force microscopy (AFM) images of the nanostructures on an Ag surface as a function of the angle of incidence of the electron beam (EB). Constant EB parameters: $U = 30$ kV; $I = 42$ pA; $d = 14$ nm; $t = 60$ s.

The results on the effects of vacuum chamber decontamination on nanostructure growth are presented in Figure 6. The nanostructures obtained before the cleaning procedure had a height of around 170 nm. The heights of the structures obtained 15 minutes after decontamination dropped to around 80 nm. Over time, the growth rate of the nanostructures gradually recovered, and 150 nm high structures were obtained two hours after the cleaning procedure.

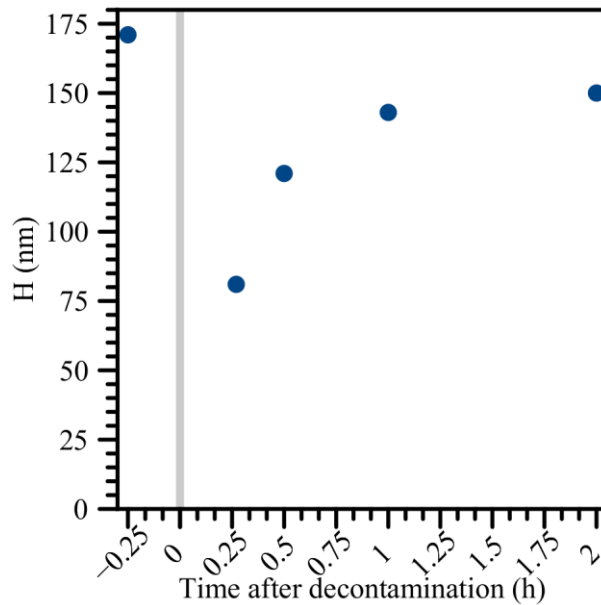


Figure 6: The height of the nanostructures on an Ag surface as a function of time following the chamber decontamination by nitrogen (N) plasma cleaning. Constant electron beam (EB) parameters: $U = 30$ kV; $I = 55$ pA; $d = 14$ nm; $t = 30$ s; $\alpha = 0^\circ$.

Discussion

Two noteworthy observations can be made according to Figure 2. The first would be the increase of nanostructure height when the EB diameter was reduced from 15 to 10 nm, while maintaining the same beam current. This observation supports the theory described in our previous work [7] regarding the movement of positive metal ions within the electric field formed around a negatively charged EB promoting nanostructure formation on metal surfaces. A smaller beam diameter would imply higher current density and stronger local electric field, resulting in larger attractive force on metal ions. The second feature is the

existence of a peak on the curve around a beam current value of 40 pA. The shape of the curve under 40 pA can be rather easily explained by the beam energy and current density. A higher beam current generally means that the electric field around the beam focus is stronger and that the beam thus supplies more energy to the surface for its deformation and the growth of structures. However, why the curve peaked and started declining at and above 40 pA is unclear. The most likely explanation would be the presence of another process which hinders the formation of nanostructures, such as for example, the radiolysis of atoms due to strikes from high energy electrons. It seems likely that interactions between the surface of the sample and high energy electrons (radiolysis, ionisation, breaking of atomic bonds) could promote the formation of nanostructures by making the surface more malleable, but as the current density was increased, these interactions could start breaking down the formed nanostructures, limiting their resulting heights.

The results presented in Figure 3 show that the height of the nanostructures on the Ag surface could be increased by elevating the EB focus by a few microns above the surface during the irradiation process. If the electric field, which causes the movement of metal ions, was centred around the focus of the EB where the negative charge density is the highest, moving the focus above the surface would have increased the electric field component in a positive direction along the z axis (Figure 1b) and resulted in increased upward movement of ions. The opposite could likely be true for moving the EB focus below the surface of the sample, besides effectively increasing the beam diameter at the surface level. The decrease of the nanostructure heights when increasing the angle of incidence of the EB, as seen in Figures 4 and 5, could be explained by a decreased component of electron energy/energy flow along the normal of the surface. The displacement of the nanostructure peaks away from EB (Figure 5, $\alpha = 10^\circ$) could be related to the destructive effects of high energy electrons at the EB's point of impact.

Regarding the problem of hydrocarbon contamination in the vacuum chamber, Figure 6 clearly shows that the presence of hydrocarbons in a vacuum chamber enhances the

growth rate of nanostructures during EB irradiation. Following the plasma cleaning procedure of the vacuum chamber, the growth rate of the nanostructures was cut by about a half and slowly recovered over time, as hydrocarbon concentrations returned to normal levels. The question now is whether the structures grown under the EB focused on metal surfaces were fully formed out of the deposited carbon or not. Carbon nanostructures formed through the EB-induced deposition of free hydrocarbons in SEM vacuum chamber have previously been described in the literature [10]. However, similarly obtained nanostructures on metal substrates containing both carbon and substrate metal have also been reported by energy dispersive X-ray spectroscopy [6]. We have previously shown that some properties of surface metal affect the size of the nanostructures formed during irradiation by a focused EB [7]. Metals with lower melting points produce higher nanostructures and metals with a higher magnetic susceptibility produce much wider structures. We have previously also reported on the creation of nanostructures exhibiting a partial shape memory effect on the surface of a shape memory alloy nitinol by irradiation with a focused EB [8]. These properties of the obtained nanostructures could not be explained through the simple deposition of carbon on a metal surface. Therefore, we conclude that the process of nanostructure formation under a focused EB is a mixed process of metal ion movement towards the negatively charged focus of the EB and the dissociation of hydrocarbons by high energy electrons and their deposition on the surface of the sample. In this work, the hydrocarbon concentrations in the SEM vacuum chamber will be considered as a constant, unless stated otherwise. Unfortunately, hydrocarbon contamination remains a difficult value to control and precisely quantify. This also means that nanostructures obtained in different devices with varying levels of carbon contamination may not exactly have the same size and purity, even if the EB beam parameters are set to be identical. On the other hand, carbon contamination in the produced nanostructures may not always represent a disadvantage, particularly if the properties of the nanostructures could be controlled and modified in a beneficial way. This, however, would require further research on the various properties (electric, magnetic, optical, and mechanical) of nanostructures obtained through irradiation by a focused EB on metal surfaces.

Conclusions

- 1) An EB current of about 40 pA results in the highest growth rate of nanostructures on Ag surfaces undergoing irradiation by a focused EB.
- 2) The growth rate of nanostructures can be enhanced by decreasing the beam diameter or by raising the beam focus a few microns above the surface of the sample.
- 3) Increasing the angle of EB incidence results in a decrease of the growth rate of the nanostructures.
- 4) If hydrocarbon contamination is present in the SEM vacuum chamber, it will be deposited on the nanostructures formed by focused EB irradiation on the Ag surface, increasing their growth rate but decreasing their purity.

Acknowledgements

This work was supported by the European Social Fund (ESF) Project No. 8.2.2.0/20/I/003 “Strengthening of Professional Competence of Daugavpils University Academic Personnel of Strategic Specialization Branches 3rd Call”

References

1. Bhushan, B. *Microelectron. Eng.* **2007**, *84*, 387-412.
2. Yeom, S.-H.; Kim, O.-G.; Kang, B.-H.; Kim, K.-J.; Yuan, H.; Kwon, D.-H.; Kim, H.-R.; Kang S.-W. *Opt. Express* **2011**, *19*, 22882-22891.
3. Lindquist, N. C.; Nagpal, P.; McPeak, K. M.; Norris, D. J.; Oh, S. H. *Rep. Prog. Phys.* **2012**, *75*, No. 036501.
4. Soh, H.T.; Quate, C.F.; Morpurgo, A.F.; Marcus, C.M.; Kong, J.; Dai, H. *Appl. Phys. Lett.* **1999**, *75*, 627-629.
5. Vieu, C.; Carcenac, F.; Pepin, A.; Chen, Y.; Mejias, M.; Lebib, A.; Manin-Ferlazzo, L.; Couraud, L.; Launois, H. *Appl. Surf. Sci.* **2000**, *164*, 111-117.

6. Ueda K.; Yoshimura. M. *Thin Solid Films*, **2004**, 464-465, 331-334.
7. Sņķeris, J.; Gerbreders, V. *Proc. SPIE*, **2017**, 10453, No. 104532B.
8. Sņķeris, J.; Gerbreders, V.; Tamanis, E. *J. Micro/Nanopattern. Mater. Metrol.* **2021**, 20(2), No. 020502.
9. Postek, M. T. *Scanning*, **2006**, 18, 269–274.
10. Zhdanov, G. S.; Manukhova, A. D.; Lozhkin, M. S. *Bull. Russ. Acad. Sci.: Phys.* **2014**, 78, 881–885.